Tetrahedron Letters 54 (2013) 431–435

Contents lists available at SciVerse ScienceDirect

Tetrahedron Letters

journal homepage: www.elsevier.com/locate/tetlet

A star-shaped sensitizer based on thienylenevinylene for dye-sensitized solar cells

Maxence Urbani [a], Eva M. Barea [b,*], Roberto Trevisan [b], Ana Aljarilla [a], Pilar de la Cruz [a], Juan Bisquert [b], Fernando Langa [a,*]

[a] Instituto de Nanociencia, Nanotecnología y Materiales Moleculares (INAMOL), University of Castilla-La Mancha., Campus de la Fábrica de Armas, Toledo 45071, Spain
[b] Photovoltaic and Optoelectronic Devices Group, Physics Department, Universitat Jaume I, Castelló 12071, Spain

ARTICLE INFO

Article history:
Received 21 September 2012
Revised 7 November 2012
Accepted 9 November 2012
Available online 23 November 2012

Keywords:
Oligothienylenevinylene
Dye-sensitized solar cell
Metal-free organic dye
Photovoltaic

ABSTRACT

A novel star-shaped dye based on highly conjugated oligothienylenevinylene (nTV) bearing pendant solubilizing hexyl chains and end-capped with three tetramethylammonium cyanoacetates as anchoring groups has been synthetized. Its photovoltaic performance, in mesoporous TiO_2 dye-sensitized solar cell, has been tested under different experimental conditions. The best performances were obtained at longer adsorption times of 4 h using different electrolyte compositions, reaching up to 3.11% of efficiency.

The global environmental issues and growing energy demand have greatly encouraged scientists and governments to explore and develop renewable and environmentally friendly energy sources. Solar photovoltaic (PV) electricity keeps growing and represents now the third source of the world-wide renewable energy in terms of installed capacity after hydro and wind power.[1] However, mainly due to the high-purity required for the inorganic silicon semiconductors in actual solar panels,[2] this technology still remains expensive in terms of price-per-KWh.

Alternative photovoltaic systems based on cheap materials and production processes such as dye-sensitized solar cells (DSCs) appear to be a promising route to produce competitive and cost-effective, new photovoltaic devices. DSCs were initially developed based on ruthenium(II)-polypyridyl complexes (such as N3, N719, or black dyes) as the active material[3] adsorbed on nanocrystalline TiO_2 with validated conversion efficiencies up to 11% under simulated AM 1.5G illumination (100 mW cm^{-2}). Metal-free organic donor–acceptor (D–A) dyes have attracted increasing attention due to their low cost, low-impact environmental pollution ('green dye'), high and tunable molar absorption coefficients, and easy modification of the molecular structures by design strategies.[4–6] A porphyrin dye has recently achieved 11% solar-to-electric power conversion efficiency at simulated 1 sun solar irradiation in combination with a Cobalt (II/III) redox couple, which is the best-efficient free-metal organic DSC to date.[7] This significant breakthrough has strongly renewed the interest and perspectives for free-metal organic based DSC.

Conjugated oligomers are target compounds for many applications in material science[8] due to their interesting optical, electrical, and optoelectronic properties. One type is star-shaped conjugated systems,[9] in which identical arms are attached to a central core. Three-armed star with a benzene core (propeller shaped)[10] has been widely used in material science as hole-blocking materials, in OLED,[11] liquid crystal,[12] as active materials for organic electronic devices such as BHJ solar cells[13] or combined with fullerene in studies of photoinduced electron transfer.[14] Finally, star-shaped systems substituted with carboxylate groups were used to produce metal-organic frameworks (MOF's).[15]

Recently we described new dyes for DSC where thienylenevinylene oligomers (nTV) of different lengths act as donor[16] or bridge[17] in D–π–A structures for DSCs. For instance, we have reported a linear 4-thienylenevynylene dye functionalized with cyanoacrylic acid as anchoring group (Chart 1) and its performance tested in mesoporous TiO_2 DSCs.[18]

We report herein on the successful synthesis and characterization of a star-shaped dye containing a benzene central core and three arms, each one formed by four thienylenevinylene oligomer units bearing pendant solubilizing hexyl chains and end-capped with three tetramethylammonium cyanoacetates as anchoring groups (Chart 2).

So far, most of the free-metal organic sensitizers previously studied and tested in DSCs are based on D–A, linear 'push–pull' type dyes. To date, very few works report on proof-to-principle

* Corresponding authors.
E-mail address: Fernando.Langa@uclm.es (F. Langa).

0040-4039/$ - see front matter © 2012 Elsevier Ltd. All rights reserved.
http://dx.doi.org/10.1016/j.tetlet.2012.11.041

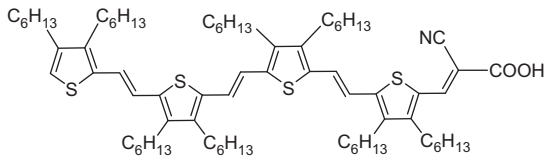

Chart 1. Molecular structure of a linear 4-thienylenevinylene dye sensitizer previously described and tested in DSCs in our group.

efficiency of multi-component, -light harvesting, and/or -anchoring dyes used in free-metal organic based DSCs, together with their structure shape relationship, such as star-shapes. To our knowledge only one example of a star-shaped molecule has been investigated as a dye for DSCs.[19] The advantage (or disadvantage) to use these kinds of multi-component systems in DSCs, covalently assembled at the supramolecular level, still remains unclear. For example we need to tune the electrolyte so that electron injection to the TiO_2 conduction band is optimal while the bulky dye structure prevents recombination by maintaining the oxidized species in the electrolyte away from the titania surface, so that the photovoltage is not reduced. These features are investigated below by determination of the electrochemical, optical, and photovoltaic properties of this new star-shaped dye and its performance in DSCs under different experimental conditions.

The synthesis of dye **6** is depicted in Scheme 1. Tris(phosphonate) **1**[20] and 4TV-CHO[21] **2** were prepared according to the procedure previously described in the literature. The first step involves the reaction of phosphonate **1** and 4TV-CHO **2** in THF with an excess of *t*-BuOK under Wittig–Horner conditions, affording triad **3** in 84% of yield. Subsequently, **3** was formylated via a Vilsmeyer–Haack reaction in the presence of an excess of $POCl_3$/DMF at reflux in DCE overnight, affording (tris)aldehyde **4** in a 71% yield. The final step was a Knoevenagel condensation with cyanoacetic acid in the presence of a catalytic amount of piperidine to convert tris–aldehyde **4** into tris–cyanoacrylic acid **5**. Due to its dual amphipathic behavior, a strong lipophilic central core induced by numerous side alkyl chains of 4TV skeletons and the hydrophylic behavior induced by the three surrounding cyanoacrylic acid polar tails, dye **5** has a strong tendency to precipitate in organic solvents such as CH_2Cl_2. In order to increase its solubility and make it more easy to handle in common organic solvents, dye **5** was converted into its (tetramethylammonium) cyanoacetate salt **6**. The structure of dye **6**, as well as its precursors **3** and **4**, was confirmed by MALDI-TOF mass spectrometry as well as ^1H and ^{13}C NMR, FT-IR, and UV–vis spectroscopies (see SI.). The thermal stability of dye **6** was studied by thermogravimetric analysis (TGA) under nitrogen, with a heating rate of 10 °C/min. Decomposition temperature (Td) was estimated as the temperature that is the intercept of the leading edge of the weight loss by the baseline of the TGA scans. Dye **6** is thermally stable with decomposition temperature higher than 378 °C (Fig. SI. 14).

The UV–visible spectra of dyes **3**, **4,** and **6** in CH_2Cl_2 are shown in Figure 1. They display the characteristic band of 4TV centered at around 545 nm. The maximum of absorption of dye **6** (549 nm, $\log\varepsilon = 4.78$) is slightly red-shifted by 11 nm compared to compounds **3** and **4** (538 nm). This can be explained by the increase of conjugation induced by the terminal cyanoacetate groups. Moreover, it can be seen a broadening of the 4TV band in dye 6, which is accompanied with a decrease of its extinction molar coefficient compared to **3** and **4** which suggests the tendency of dye **6** to form aggregates in organic solution. It is interesting to note that the absorption of **6** covers up to 700 nm, facilitating the absorption in this region of the solar emission. Utilization of materials that absorb light extending into the infrared range is one of the strategies to harvest more solar light and thereby to increase power-efficiency.[22] The high molar extinction coefficient absorption bands are as well in favor of light harvesting and hence photocurrent generation.

The fluorescence emission spectroscopy was employed to get information about the excited state-solvent interactions. The emission maxima of dye **6** can be found at 750 nm (λ_{exc} = 549 nm) (Fig. SI.13). The optical band gap for dye **6** is 1.96 eV, and it was calculated by the intersection of absorption and emission spectra. The large Stokes shift of dye **6** (201 nm) can be attributed to the significant structural reorganization upon photoexcitation or to the charge transfer nature of the excited state. Upon adsorption onto TiO_2 the emission was totally quenched indicating an efficient photoinduced electron transfer process from dye **6** to the TiO_2 nanoparticles.

The redox properties of dye **6** were investigated through Cyclic Voltammetry (CV) and Osteryoung Square Wave Voltammetry

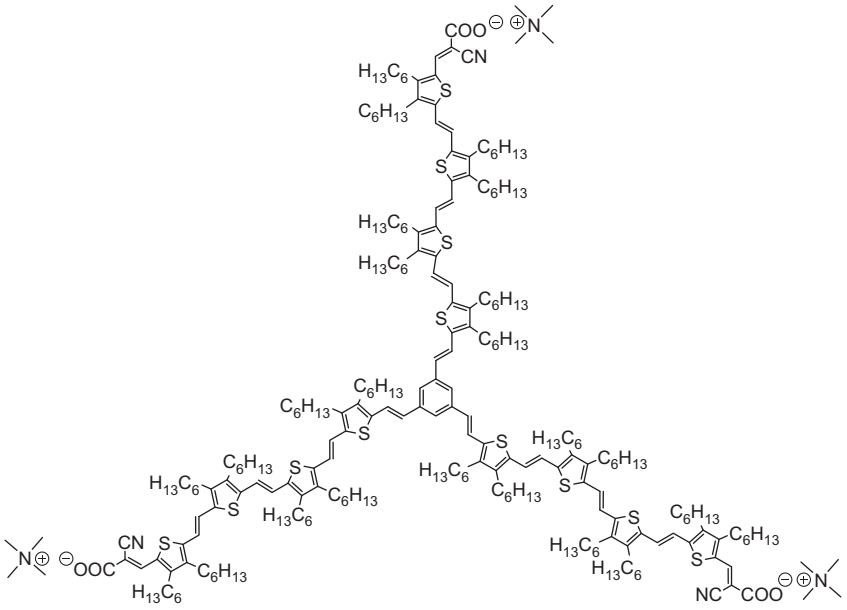

Chart 2. Molecular structure of the novel star-shaped sensitizer based on 4-thienylenevinylene studied in this work (dye 6).

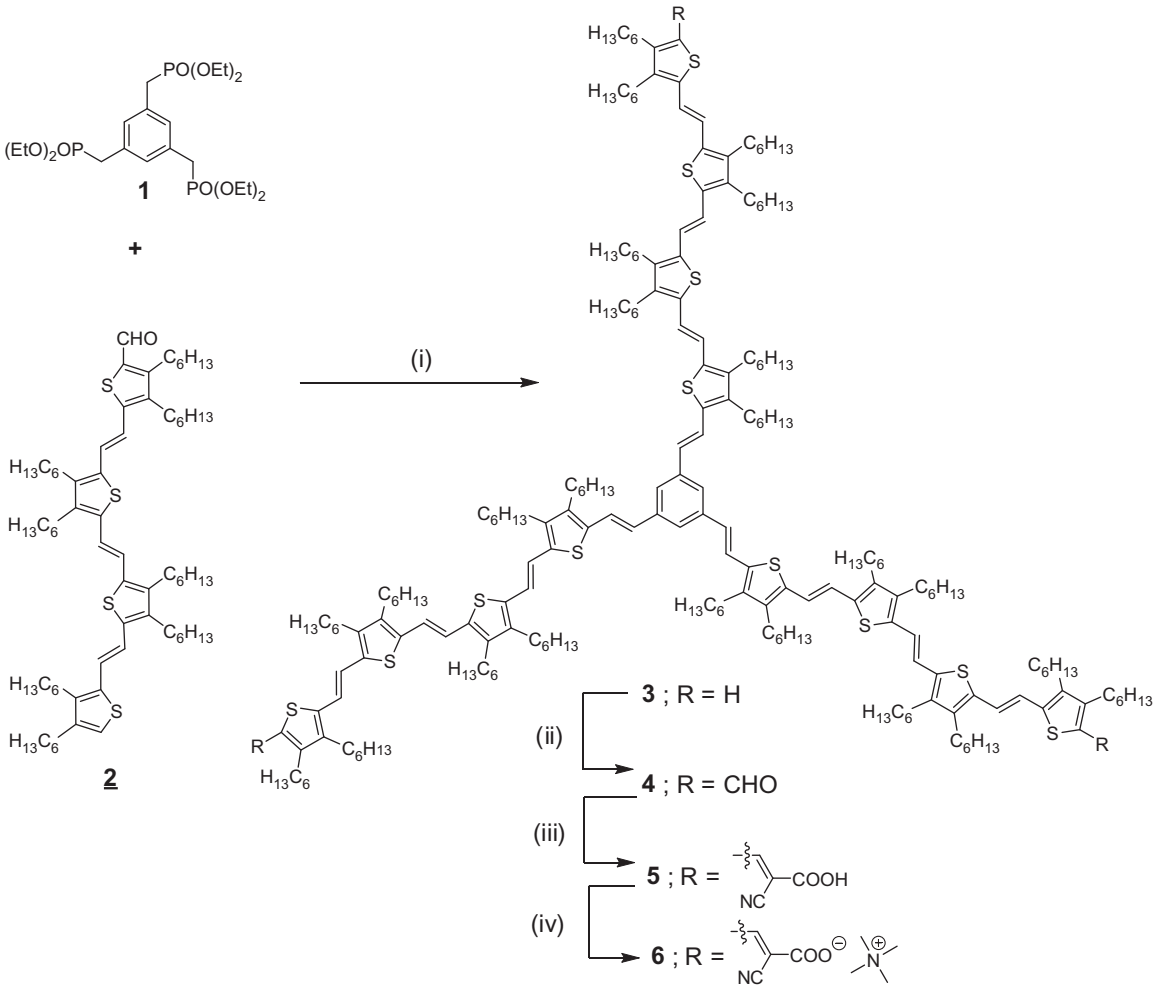

Scheme 1. Synthesis of dye 6. Reagents and conditions: (i) *t*-BuOK, THF, 0° → 20 °C, 3 h (84%), (ii) DMF, $POCl_3$, DCE, reflux overnight (71%), (iii) Cyanoacetic acid, piperidine, $CHCl_3$, reflux 24 h (83%), (iv) $N(CH_3)_4OH/H_2O$ (quantitative).

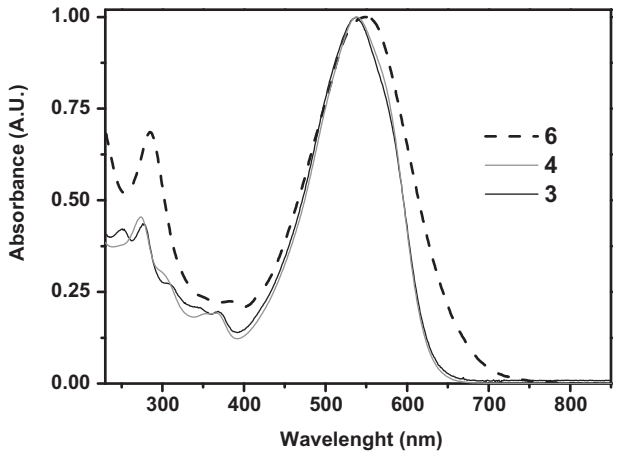

Figure 1. Normalized UV–visible spectra of dyes 3, 4, and 6 in dichloromethane.

(OSWV) at room temperature in o-dichlorobenzene:acetonitrile (4:1). Dye **6** undergoes a broad oxidation process (Fig. SI.15); the deconvolution of this broad process showed two stable and reversible (according to CV) radical cations, at 0.18 and 0.32 V (vs Fc/Fc^+, Fig. SI.15) assigned to the triple oxidation of the three 4TV arms of the dye by comparison with a sample of 4TV-COOH. The HOMO value (calculated with respect to ferrocene, HOMO: −5.1 eV)[23] was determined as −5.28 eV. In the cathodic side, a reduction process is observed at −1.96 V which we attribute to the cyanoacrylic moieties (Fig. SI.16). The LUMO value was determined as −3.14 eV.

To gain insight into the geometry and the electronic structures of the frontier orbitals, the more stable conformation and the electron density distributions of HOMO and LUMO have been calculated using DFT on B3LYP 6-31G level in the gas phase with GAUSSIAN 03W. DFT optimized gas-phase geometries of **5** have a totally planar backbone (Fig. 2) with a HOMO well delocalized over the molecules (Fig. SI.17). LUMO coefficients are mostly concentrated on the cyanoacrylic groups.

Theoretical calculations suggest that each arm in the dye behaves as an isolated chromophore with little electronic interaction between the arms as the occupied orbitals, the HOMO, HOMO−1, and HOMO−2, are threefold degenerated as well as the unoccupied orbitals (LUMO, LUMO+1, LUMO+2). The electronic distribution of compound **5** should be a sum of all these orbitals.

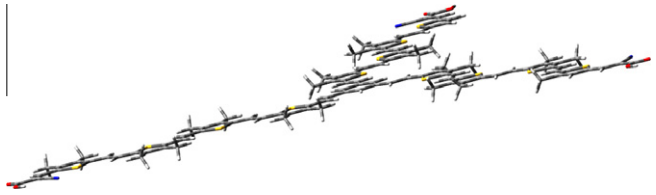

Figure 2. B3LYP/3-21G optimized structure of compound **5**.

Table 1
Photovoltaic performance obtained for dye 6

Electrolyte	Adsorption time (h)	V_{oc}[a] (V)	J[b] (mA/cm^2)	FF[c]	η[d]
E5	1	0.42	5.83	0.60	1.48
E5	2	0.45	9.24	0.58	2.43
E5	4	0.47	11.50	0.58	**3.11**[e]
F1	1	0.60	0.59	0.77	0.27
F1	2	0.61	0.67	0.76	0.31
F1	4	0.64	0.78	0.78	0.39
N7	1	0.54	4.65	0.68	1.70
N7	2	0.56	5.06	0.71	2.00
N7	4	0.44	11.60	0.60	**3.05**[e]

[a] Open circuit potential voltage.
[b] Short circuit photocurrent density.
[c] Fill factor.
[d] Power conversion efficiency.
[e] Best efficiences.

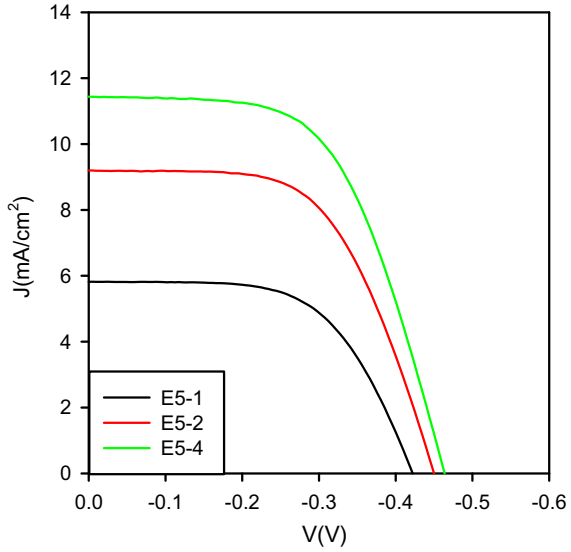

Figure 3. Current density-potential curves for DSCs at 1 sun with dye 6 as sensitizers after 1, 2, 4 h of adsorption using E5 as the electrolyte. (−1, −2, −4 are the adsorption times).

The photovoltaic performance of solar cells based on dye **6** under AM 1.5G illumination (100 mW cm^{-1}), was tested using three different electrolyte compositions (named E5, F1 and N7) and varying the adsorption time (1, 2 and 4 h). The results, obtained from an average of five samples per experiment, are summarized in Table 1 and the J–V curves are shown in Figures 3 and 4 and Figure SI.18. The composition of the different electrolytes used are: (1) Electrolyte E5: [LiI] = 0.5 M, [I_2] = 0.05 M in 3-methoxypropionitrile. (2) Electrolyte F1: [guanidine thiocyanate] = 0.1 M, [I_2] = 0.03 M, [1-butyl-3-methylimidazolium iodide] = 0.6 M, and [4-tert-butylpyridine] = 0.5 M in acetonitrile:valeronitrile (85:15) v/v. (3) Electrolyte N7: [LiI] = 0.5 M, [I_2] = 0.05 M, and [1-methylbenzimidazole] = 0.5 M in 3-methoxypropionitrile. The reason to adopt a variety of electrolytes is to modify the conduction band and the surface properties of titania in order to obtain optimal injection and photovoltaic parameters for this specific dye.

In all our experiments the same trend has been observed for the three electrolytes used: longer adsorption times result in a strong increase of the current density and therefore of the overall efficiency of the cells, due to large amount of adsorbed dye. The best efficiencies were obtained after four hours of adsorption time using E5 and N7 as electrolytes, reaching 3.11 and 3.05%, respectively.

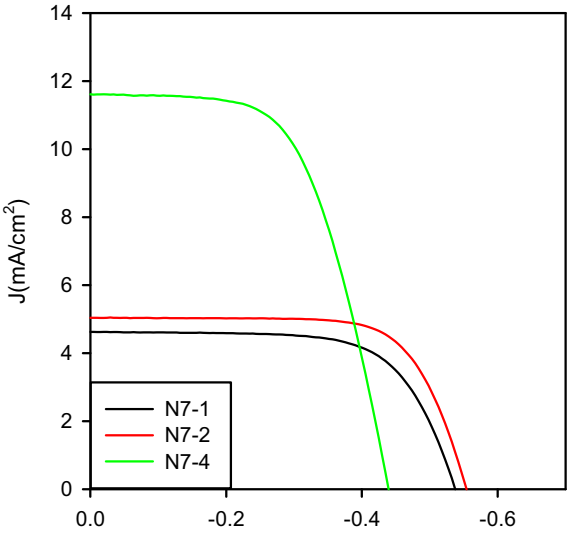

Figure 4. Current density-potential curves for DSCs at 1 sun with dye 6 as sensitizers after 1, 2, 4 h of adsorption using N7 as the electrolyte. (−1, −2, −4 are the adsorption times).

Absorption time, longer than 4 h, gives as a result a strong decrease in the performance (data not shown), probably due to strong aggregation problems. Even the use of a co-adsorbent (chenodeoxycholic acid) does not improve the performance of the cells, obtaining similar results. Both electrolytes are quite similar, containing N7 1-methylbenzimidazole (MBII) that keep the titania conduction band lightly shift up, obtaining around 0.54–0.56 V circuit voltage (V_{oc}) compared with the voltage values obtained for E5 electrolyte without MBII. For all the cells the efficiency increases with longer absorption time (been four h the optimum time).

Surprisingly, extremely poor efficiencies (0.27–0.39%) were obtained with F1 electrolyte (without LiI, and containing ionic liquid and different solvents). We explain this result by a strong upward displacement of the TiO_2 conduction band respecting that in the case of electrolyte F1, due to the ionic liquid and the lack of LiI, which strongly disfavors the electron injection from the LUMO of dye **6** and consequently very low values are obtained for J_{sc}.[24] This is also reflected by the higher V_{oc} values obtained with F1 electrolyte (V_{oc} ≈−0.6 V) than with N7 and E5 (V_{oc} ≈−0.5 and −0.4 V respectively).

In conclusion, we have successfully synthesized a star-shaped dye containing a benzene central core and three arms, each one formed by four thienylenevinylene oligomer units bearing pendant solubilizing hexyl chains and end-capped with three tetramethylammonium cyanoacetates as anchoring groups. Its optical and electrochemical properties were studied and a DSC device was manufactured; the overall conversion of this device appeared to be strongly dependent on the electrolyte used. The highest values of photocurrent and consequently the highest efficiencies, were obtained using E5 and N7 as electrolytes with a maximum of 3.11%.

Acknowledgments

Financial support from the Ministerio de Ciencia y Tecnología of Spain (Projects and Consolider Project HOPE-CSD2007-00007, MAT2010-19827 and CTQ2010-1749), JCCM and FEDER funds (Project POII09-0078-923) is gratefully acknowledged. UJI work is also supported by the 'Institute of Nanotechnologies for Clean Energies', funded by the Generalitat Valenciana under project ISIC/2012/008 and PROMETEO/2009/058.

Supplementary data

Supplementary data associated with this article can be found, in the online version, at http://dx.doi.org/10.1016/j.tetlet.2012.11.041.

References and notes

1. (a) Annual report 2011, 2012, European Photovoltaic industry association.; (b) Global Market Outlook for Photovoltaics until 2016, 2012, European Photovoltaic industry association.
2. (a) Hagfeldt, A.; Gratzel, M. *Acc. Chem. Res.* **2000**, *33*, 269–277; (b) Grätzel, M. *Inorg. Chem.* **2005**, *44*, 6841–6851.
3. (a) Grätzel, M. *Acc. Chem. Res.* **2009**, *42*, 1788–1798; (b) Cao, Y.; Bai, Y.; Yu, Q.; Cheng, Y.; Liu, S.; Shi, D.; Gao, F.; Wang, P. *J. Phys. Chem. C* **2009**, *113*, 6290–6297; (c) Hagfeldt, A.; Boschloo, G.; Sun, L. C.; Kloo, L.; Pettersson, H. *Chem. Rev.* **2010**, *110*, 6595–6663.
4. Mishra, A.; Fischer, M. K. R.; Bauerle, P. *Angew. Chem., Int. Ed.* **2009**, *48*, 2474–2499.
5. Ooyama, Y.; Harima, Y. *Eur. J. Org. Chem.* **2009**, 2903–2934.
6. Fitzner, R.; Mena-Osteritz, E.; Mishra, A.; Schulz, G.; Reinold, E.; Weil, M.; Korner, C.; Ziehlke, H.; Elschner, C.; Leo, K.; Riede, M.; Pfeiffer, M.; Uhrich, C.; Bauerle, P. *J. Am. Chem. Soc.* **2012**, *134*, 11064–11067.
7. (a) Tour, J. M. *Chem. Rev.* **1996**, *96*, 537–554; (b) Meier, H. *Angew. Chem., Int. Ed.* **2005**, *44*, 2482–2506.
8. Yella, A.; Lee, H.-W.; Tsao, H. N.; Yi, C.; Chandiran, A. K.; Nazeeruddin, M.; Diau, E. W.-G.; Yeh, C.-Y.; Zakeeruddin, S. M.; Grätzel, M. *Science* **2011**, *334*, 629–634.
9. Detert, H.; Lehmann, M.; Meier, H. *Materials* **2010**, *3*, 3218–3330.
10. (a) Schmidt, B.; Rinke, M.; Güsten, H. *J. Photochem. Photobiol., A* **1989**, *49*, 131–135; (b) Yamaguchi, Y.; Ochi, T.; Miyamura, S.; Tanaka, T.; Kobayashi, S.; Wakamiya, T.; Matsubara, Y.; Yoshida, Z. *J. Am. Chem. Soc.* **2006**, *128*, 4504–4505.
11. Lu, J. P.; Tao, Y.; D'iorio, M.; Li, Y. N.; Ding, J. F.; Day, M. *Macromolecules* **2004**, *37*, 2442–2449.
12. Sergeyev, S.; Pisula, W.; Geerts, Y. H. *Chem. Soc. Rev.* **2007**, *36*, 1902–1929.
13. (a) Unger, E. L.; Ripaud, E.; Leriche, P.; Cravino, A.; Roncali, J.; Johansson, E. M. J.; Hagfeldt, A.; Boschloo, G. *J. Phys. Chem. C* **2010**, *114*, 11659–11664; (b) Lin, Z.; Bjorgaard, J.; Yavuz, A. G.; Köse, M. E. *J. Phys. Chem. C* **2011**, *115*, 15097–15108.
14. Pérez, L.; García-Martínez, J. C.; Díez-Barra, E.; García, H.; Rodríguez-López, J.; Langa, F. *Chem. Eur. J.* **2006**, *12*, 5149–5157.
15. Sun, D.; Ke, Y.; Mattox, T. M.; Parkin, S.; Zhou, H. *Inorg. Chem.* **2006**, *45*, 7566–7568.
16. Caballero, R.; Barea, E. M.; Fabregat-Santiago, F.; de la Cruz, P.; Márquez, L.; Langa, F.; Bisquert, J. *J. Phys. Chem. C* **2008**, *112*, 18623–18627; (b) Mora-Seró, I.; Gros, D.; Dittereder, T.; Lutich, A. A.; Susha, A. S.; Dittrich, T.; Belaidi, A.; Caballero, R.; Langa, F.; Bisquert, J.; Rogach, A. L. *Small* **2010**, *6*, 221–225.
17. (a) Clifford, J. N.; Forneli, A.; López-Arroyo, L.; Caballero, R.; de la Cruz, P.; Langa, F.; Palomares, E. *ChemSusChem* **2009**, *2*, 344–349; (b) Barea, E. M.; Caballero, R.; López-Arroyo, L.; Guerrero, A.; de la Cruz, P.; Langa, F. *ChemPhysChem* **2011**, *12*, 961–965.
18. Barea, E. M.; Caballero, R.; Fabregat-Santiago, F.; de la Cruz, P.; Langa, F.; Bisquert, J. *ChemPhysChem* **2010**, *11*, 245–250.
19. (a) Johansson, P. G.; Zhang, Y.; Abrahamsson, M.; Meyer, G. J.; Galoppini, E. *Chem. Commun.* **2011**, *47*, 6410–6412; (b) Persson, P.; Knitter, M.; Galoppini, E. *RSC Adv.* **2012**, *2*, 7868–7874; (c) Chitre, K. P.; Guillén, E.; Yoon, A. S.; Galoppini, E. E. *J. Inorg. Chem.* **2012**. http://dx.doi.org/10.1002/ejic.201200896; (d) Duan, T.; Fan, K.; Fu, Y.; Zhong, C.; Chen, X.; Peng, T.; Qin, J. *Dyes Pigm.* **2012**, *94*, 28–33.
20. Díez-Barra, E.; García-Martínez, J. C.; Merino, S.; del Rey, R.; Rodríguez-López, J.; Sánchez-Verdú, P.; Tejeda, J. *J. Org. Chem.* **2001**, *66*, 5664–5670.
21. Synthesized according to the procedure described in the literature: (a) Jestin, I.; Frère, P.; Mercier, N.; Levillain, E.; Stievenard, D.; Roncali, J. *J. Am. Chem. Soc.* **1998**, *120*, 8150–8158; (b) Oswald, F.; Islam, D.-M. S.; Araki, Y.; Troiani, V.; de la Cruz, P.; Ito, O.; Langa, F. *Chem. Eur. J.* **2007**, *13*, 3924–3933.
22. (a) Langa, F.; de la Cruz, P.; Espíldora, E.; de la Hoz, A.; Bourdelande, J.; Sanchez, L.; Martin, N. *J. Org. Chem.* **2001**, *66*, 5033–5041; (b) Wang, X.; Perzon, E.; Delgado, J. L.; de la Cruz, P.; Zhang, F.; Langa, F.; Andersson, M. R.; Inganäs, O. *Appl. Phys. Lett.* **2004**, *85*, 5081–5083; (c) Wang, X.; Perzon, E.; Oswald, F.; Langa, F.; Admassie, S.; Andersson, M. R.; Inganäs, O. *Adv. Funct. Mater.* **2005**, *15*, 1665–1670.
23. Cardona, C. M.; Li, W.; Kaifer, A. E.; Stockdale, D.; Bazan, G. C. *Adv. Mater.* **2011**, *23*, 2367–2371.
24. (a) Barea, E. M.; Ortiz, J.; Pay, F. J.; Fernández-Lázaro, F.; Fabregat-Santiago, F.; Sastre-Santos, A.; Bisquert, J. *Energy Environ. Sci.* **2010**, *3*, 1985–1994; (b) Barea, E. M.; Zafer, C.; Gultekin, B.; Aydin, B.; Koyuncu, S.; Icli, S.; Fabregat-Santiago, F.; Bisquert, J. *J. Phys. Chem. C* **2010**, *114*, 19840–19848; (c) Barea, E. M.; González-Pedro, V.; Ripollés-Sanchis, T.; Wu, H.-P.; Li, L.-L.; Yeh, C.-Y.; Diau, E. W.-G.; Bisquert, J. *J. Phys. Chem. C* **2011**, *115*, 10898–10902.